BOLLETTINO DI GEOFISICA TEORICA ED APPLICATA VOL. 40, N. 2, pp. 95-110; JUNE 2000

Ground displacement in a fault zone in the presence of asperities

S. SANTINI[(1)], A. PIOMBO[(2)] and M. DRAGONI[(2)]

[(1)] *Istituto di Fisica, Università di Urbino, Italy*
[(2)] *Dipartimento di Fisica, Settore di Geofisica, Università di Bologna, Italy*

(Received June 24, 1999; accepted May 17, 2000)

Abstract. Friction on faults controls slip distribution in response to tectonic stress: the friction distribution can be simplified by considering locked zones (asperities) surrounded by aseismic slipping zones. The aseismic slip of fault sections has an important role in concentrating stress on the asperities and in producing their failure. The slow ground displacement in fault zones is measurable through classic or spatial geodetic techniques and may help to localize the greater asperities on faults. Therefore accurate geodetic measurements in fault zones may be used to evaluate the seismic hazard in the region. We represent the Earth's crust by an elastic, homogeneous and isotropic half-space, including a plane normal fault. A locked asperity is considered on the fault, while the surrounding area of the fault surface undergoes a uniform slip. The surface displacement field is analyzed in the presence and in the absence of the asperity; the influence of the asperity shape, size and depth is studied also varying the dip angle of the fault. We conclude that an asperity, whose area is about 1 km^2, determines a surface displacement of mm order, when its centre is placed at depths ranging from 5 to 10 km and the surrounding fault area slips by tens of centimeters: in this case an asperity with an area of about 5×5 km^2 could be reasonably localized by current geodetic measurements.

1. Introduction

Earthquakes result when the Earth's crust fails in response to accumulated deformation. Geodetic measurements document the crustal deformation leading to these failures and the deformation resulting from them. For both earthquakes and aseismic fault motions, geodetic

Corresponding author: M. Dragoni; Dipartimento di Fisica, Settore di Geofisica, Università di Bologna, Viale B. Pichat 8, Bologna, Italia; phone: +39 02 23996504; fax +39 02 23996530; e-mail: dragoni@ibogfs.df.unibo.it

measurements constrain physical models of the processes that cause such events.

The use of leveling, GPS and SAR interferometry (InSAR) data allows us to determine the displacement field at the Earth's surface associated with fault slip. In particular, whereas measurements by conventional and space-based geodetic methods, such as GPS, can more accurately determine the displacement vectors for a network of points, InSAR can provide much denser spatial coverage of the ground displacement.

The observed variability in the seismic phenomenology is attributed to the mechanic heterogeneity of the fault surfaces. The asperity model of faults assumes that earthquakes are a consequence of the fast failure of one or more asperities, occurring when the tectonic stress, increasing over a long period of time, overcomes the resistance of the asperity. The search for asperities on active faults is therefore a fundamental step towards a deeper understanding of the seismic source and its dynamics.

Several methods can be used to recognize and locate asperities: the measurement of ground deformation; the observation of seismicity patterns; the analysis of seismic records of past earthquakes (both strong motions and teleseismic waves); and, in particular cases, geologic observations.

If the study of seismicity provides basic information about the failure of strong fault patches, only the observation of slow ground deformation can give direct information about areas which slip aseismically. In fact, it is conceivable that in the time interval between two large earthquakes on the same fault segment (interseismic phase), the relative plate motion along a plate boundary is partly accommodated by the aseismic slip of faults. The contrast between the locked areas (asperities) and the freely slipping areas on a fault surface is detectable at the Earth's surface by geodetic techniques. Therefore, ground deformation measurements can play a crucial role in the search for asperities, in particular if part of the interseismic slip is aseismic.

Attempts to recognize asperities on the San Andreas Fault, in particular on the Parkfield segment, were made by several authors (Slawson and Savage, 1983; Bakun and Lindh, 1985; Stuart et al., 1985; Tse et al., 1985; Harris and Segall, 1987; Stuart and Tullis, 1995).

In order to evaluate the pattern and magnitude of ground deformation due to asperities, Dragoni (1988) considered a model in which asperities of different shapes, sizes and depths are present on a vertical strike-slip fault embedded in an elastic half-space. In this paper in order to improve the interpretation of geodetic measurements in terms of asperities for a wider number of situations, we calculate the displacement and tilt fields produced by the presence of asperities on normal faults with different dip angles, embedded in an elastic half-space. Such a model could be usefully employed for the seismogenic structures of the Apenninic chain, where an increasing amount of geodetic data is becoming available.

2. The model

Let us consider an elastic, homogeneous and isotropic half-space, occupying the region $x_3 \leq 0$ in a Cartesian coordinate system (Fig. 1a), and assume that a half-plane represents a normal fault surface intersecting the Earth's surface with a dip angle δ. As is usual for the Earth's crust, it is

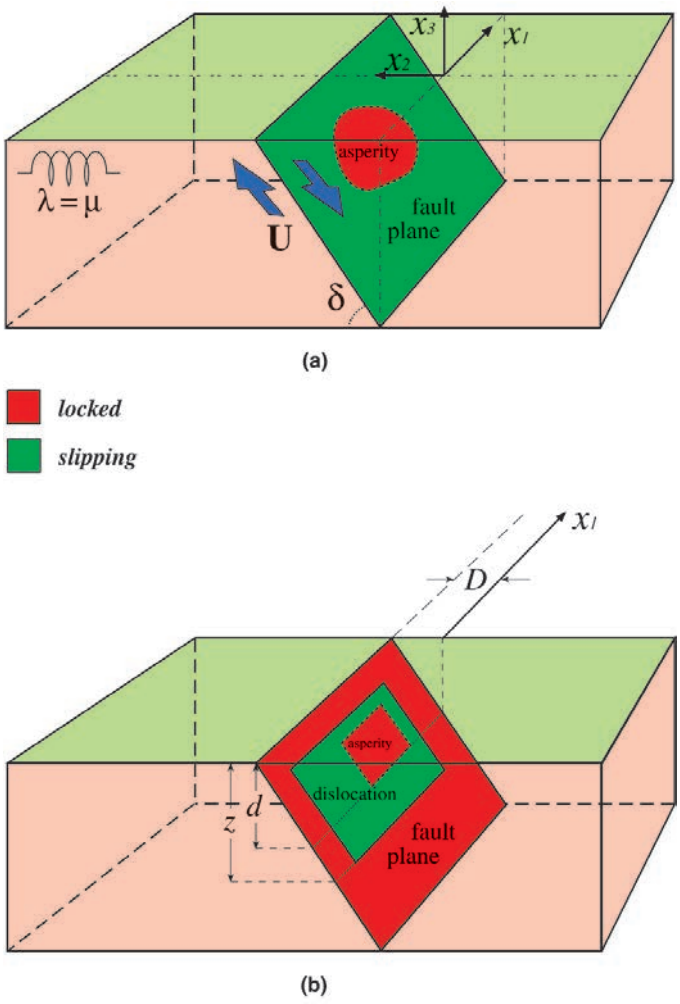

Fig. 1 - (a) The model: the green area indicates a slipping zone on a normal fault and the red one a locked zone (asperity). (b) Case of a finite-area dislocation including an asperity: z is the depth of the bottom size of the dislocation, d is the same quantity for the asperity and D is the distance of fault trace from the x_1 axis.

assumed that the Lamé constants are equal (Poisson solid) and $\lambda=\mu=3\times10^{10}$ Pa. In the case of a rectangular dislocation, the displacement field at the Earth's surface can be obtained by available analytical solutions (e.g. Okada, 1985). The x_1 axis is parallel to the fault strike and contains the projection of the bottom side of the dislocation on the Earth's surface.

It is assumed that friction on the fault is not homogeneous, but that asperities are present. According to the asperity model, during the interseismic phase, the fault slips aseismically or with small earthquakes, corresponding to smaller asperity failures. We assume that a single dominant asperity is present on the fault: this asperity remains locked, while the remaining part of the fault slips aseismically in a uniform fashion by an amount U. The displacement field produced by dislocations, including asperities, can be obtained by suitably combining solutions for dislocations.

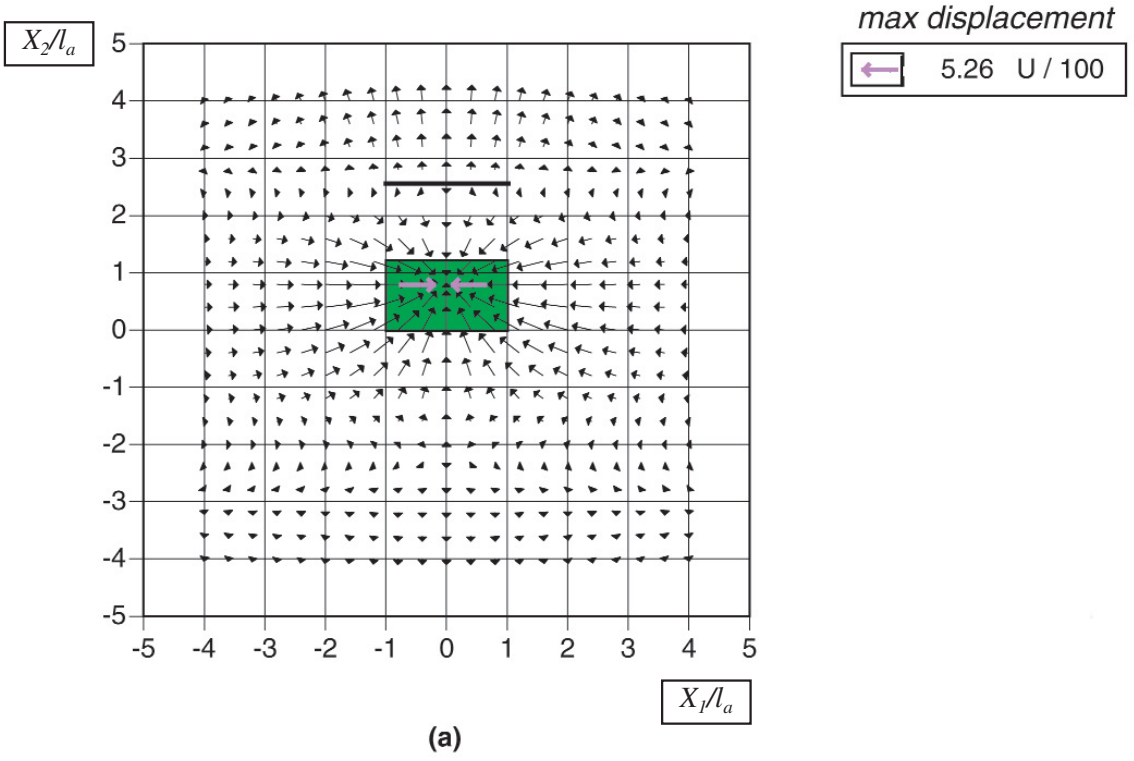

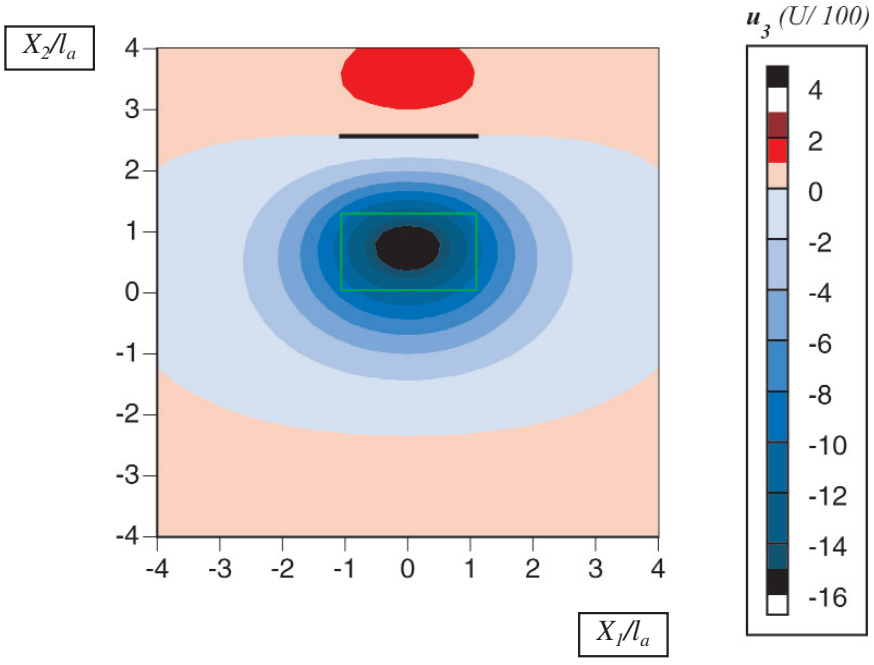

Fig. 2 - Ground displacement due to a finite-area dislocation with z = 15 km, δ = 50° and l_d = 5 km: (a) map of horizontal displacement; (b) map of vertical displacement.

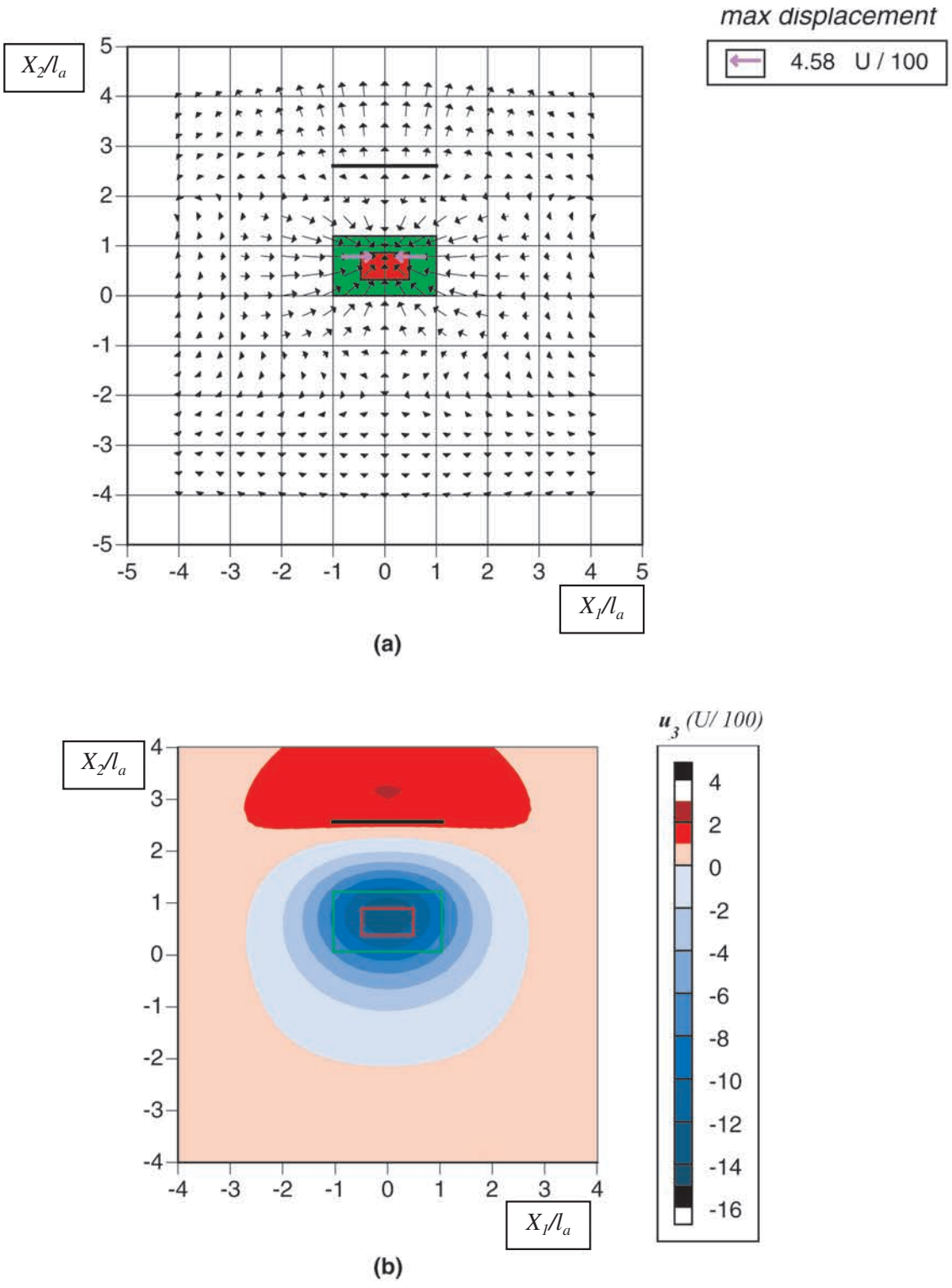

Fig. 3 - Ground displacement due to a finite-area dislocation with z = 15 km, δ = 50° and l_d = 5 km, including a concentric square asperity with l_a = 2.5 km: (a) map of horizontal displacement; (b) map of vertical displacement.

We consider asperities and dislocations with rectangular shapes and find the solutions in the presence of asperities by considering the asperity as a fault region where the slip is opposite to that of the dislocation (Fig. 1b). We call z the depth of the bottom side of dislocations and d the same quantity for asperities. For simplicity, we examine the case of a square dislocation and a square asperity having the same centre.

We indicate with $\boldsymbol{u}^d\ (x_1, x_2; U, l_d)$ the ground displacement in the case of a square dislocation with a side of half-length l_d and a slip amplitude U; accordingly, the effect of a square asperity with a side of half-length l_a can be indicated as $\boldsymbol{u}^d\ (x_1, x_2; -U, l_a)$. Since U is a multiplying factor in the displacement, one can write

$$\boldsymbol{u}^d(x_1,\ x_2;\ -U,\ l_a) = -\boldsymbol{u}^d(x_1,\ x_2;\ U,\ l_a) \tag{1}$$

The total displacement field at the Earth's surface is obtained by adding the contributions of the dislocation and the asperity:

$$\boldsymbol{u}\ (x_1,\ x_2) = \boldsymbol{u}^d(x_1,\ x_2;\ U,\ l_a) - \boldsymbol{u}^d(x_1,\ x_2;\ U,\ l_a) \tag{2}$$

In the case of a square asperity on a half-plane fault, the displacement components $\boldsymbol{u}_2$ and $\boldsymbol{u}_3$ are obtained by adding a uniform slip of the fault walls to the corresponding components of ground displacement due to the asperity:

$$u_2\ (x_1,\ x_2) = \begin{cases} \dfrac{U}{2}\sin d - u_2^d(x_1,\ x_2;\ U,\ l_a) & x_2 > D \\ -\dfrac{U}{2}\sin\ d - u_2^d(x_1,\ x_2;\ U,\ l_a) & x_2 < D \end{cases} \tag{3}$$

$$\boldsymbol{u}_3\ (x_1,\ x_2) = \begin{cases} \dfrac{U}{2}\sin\ \delta - \boldsymbol{u}_3^d(x_1,\ x_2;\ U,\ l_a) & x_2 > D \\ -\dfrac{U}{2}\sin\ \delta - \boldsymbol{u}_3^d(x_1,\ x_2;\ U,\ l_a) & x_2 < D \end{cases} \tag{4}$$

where D is the distance from the x_1 axis to the fault trace

$$D = d\ \ \text{cotan}\ \ \delta \tag{5}$$

The component x_1 is given by

$$\boldsymbol{u}_1\ (x_1,\ x_2) = \boldsymbol{u}_1^d(x_1,\ x_2;\ U,\ l_a) \tag{6}$$

Another useful quantity to be measured at the Earth's surface is ground tilt, the components of which are defined as

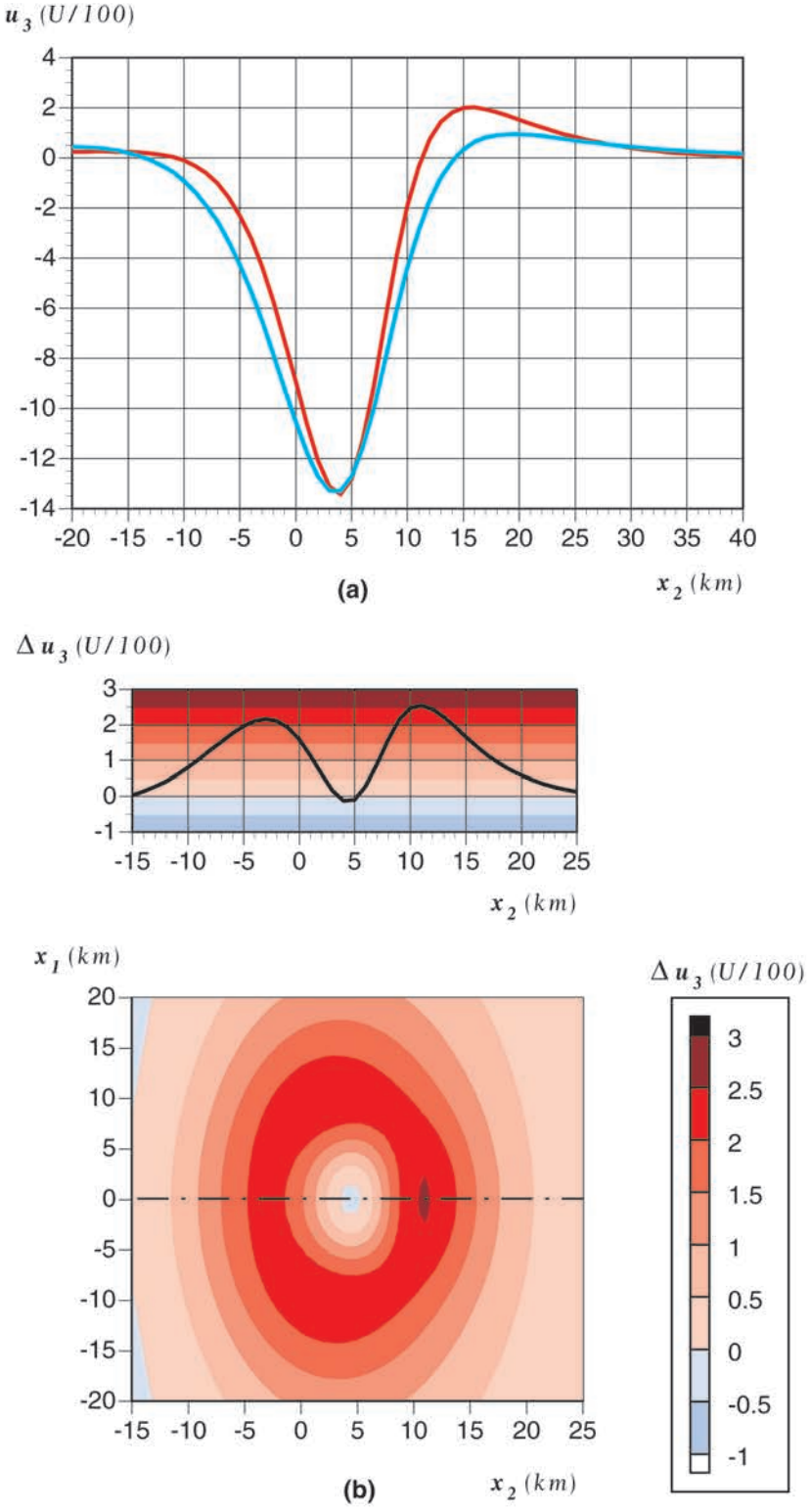

Fig. 4 - (a) Curves of u_3 component along the x_2 axis for the case of Fig. 3 (red) and for an appropriate dislocation of smaller area without asperity (blue) (for parameters see text).

$$t_i = \frac{\partial u_3}{\partial x_i} \quad i = 1,2 \tag{7}$$

From the solution for a square asperity, it is easy to obtain the analytical solution for any asperity, with a polygonal contour. As a consequence, it is possible to model the presence of asperities with any shape.

3. Discussion

To evaluate the effect on ground displacement of the presence of an asperity on a fault plane, first we consider the displacement field due to a square dislocation; secondly, we examine the case when an asperity is present inside the dislocation. In Fig. 2, the components of displacement produced by a square dislocation are shown for $\delta = 50°$, $l_d = 5$ km and $z = 15$ km; in Fig. 3 the displacement field produced by the same dislocation, including a square asperity of side $l_a = 2.5$ km, is shown. Note that vertical displacement reaches its maximum values along the x_2 axis. Negative values of vertical displacement indicate subsidence and positive values indicate uplift, since the x_3 axis points upward. The presence of an asperity in the dislocation produces an increase of the area which is affected by significant uplift, but a decrease of the maximum vertical displacement. For $U = 50$ cm, the maximum displacement in the case of Fig. 2 is about 8 cm and in the case of Fig. 3 is about 7 cm. The maximum absolute values of ground displacement are found in correspondence to the centre of the projection on the Earth's surface of the dislocation.

Because the aim of this paper is the interpretation of geodetic measurements, in the following we consider the vertical displacement field along the x_2 axis where u_3 is maximum.

It is interesting to evaluate whether the effects of an asperity inside a dislocation can be modeled by a dislocation with a smaller area but without asperity. Fig. 4a shows that the vertical displacement along the x_2 axis, for the case in Fig. 3, has the same minimum value as that due to a concentric dislocation with $l_d = 4.55$ km but without asperity. The presence of an asperity causes a different $u_3$pattern and in particular a shift from the fault trace of the position of maximum uplift. Since geodetic measurements can have centimetre point positioning accuracies from several millimetres to 1 cm, the difference between the two curves of Fig. 4a must be at least of this magnitude for an appropriate interval of x_2 in order to distinguish between the two different situations. Fig. 4b shows that it can be achieved for an amount of slip of 50 cm and that there are two regions along the x_2 axis, 3 and 5 km wide respectively, where the difference between two cases can be measured.

In the case of a half-plane dislocation, Fig. 5 shows the displacement field for an asperity with $d = 15$ km, $l_a = 2.5$ km, $\delta = 45°$; Fig. 6 shows the same case but for $d = 10$ km. We note that the pattern of ground displacement varies appreciably, but the maximum values are about constant. As expected, the area of maximum displacement increases for decreasing asperity depths.

We can conclude that the presence of an asperity on a fault plane may change the ground displacement field appreciably and, in favourable cases, can allow the location of locked patches.

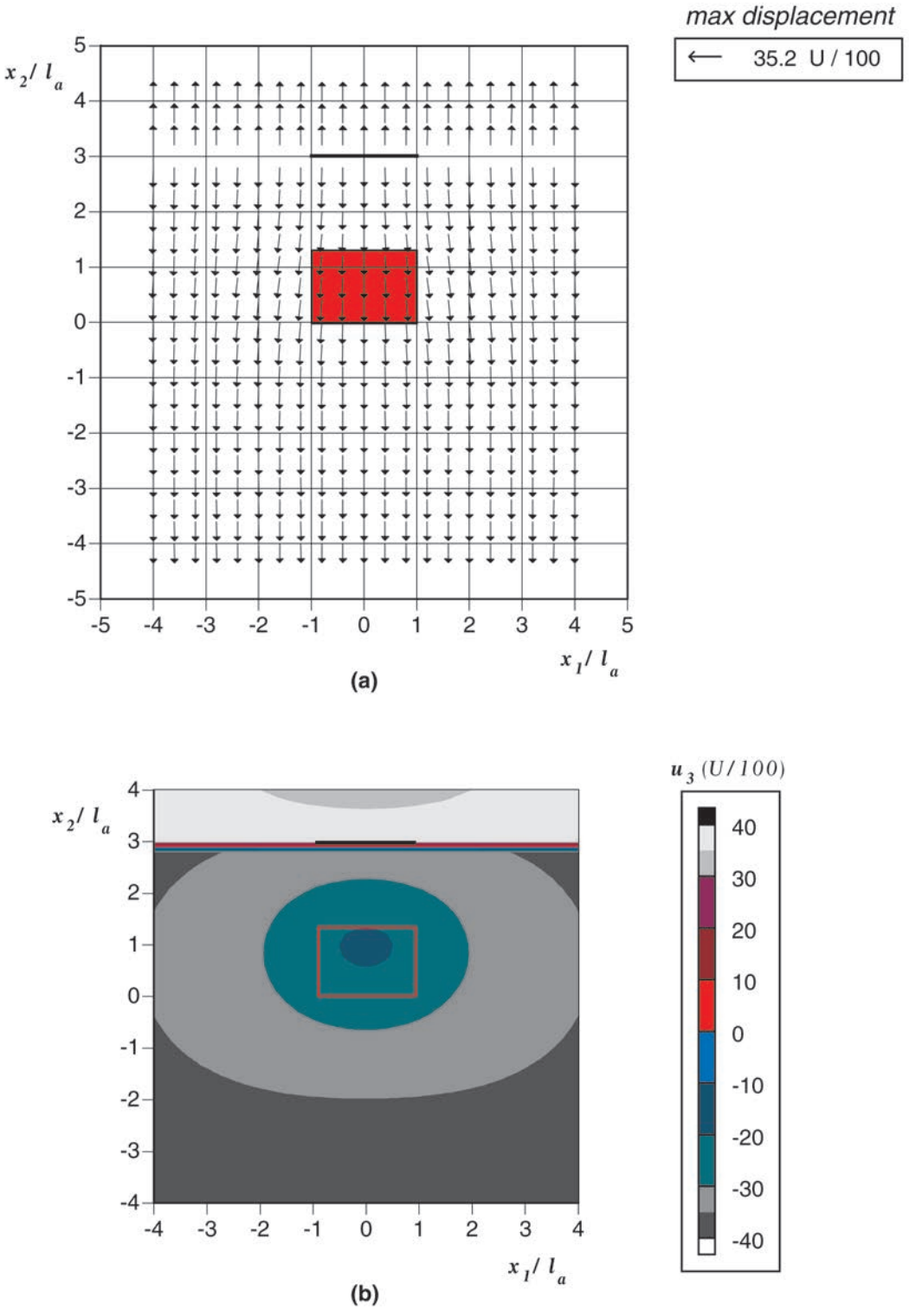

Fig. 5 - Maps of horizontal (a) and vertical displacement (b) in the case of an asperity included in a half-plane dislocation: z = 15 km, δ = 45° and l_a = 5 km.

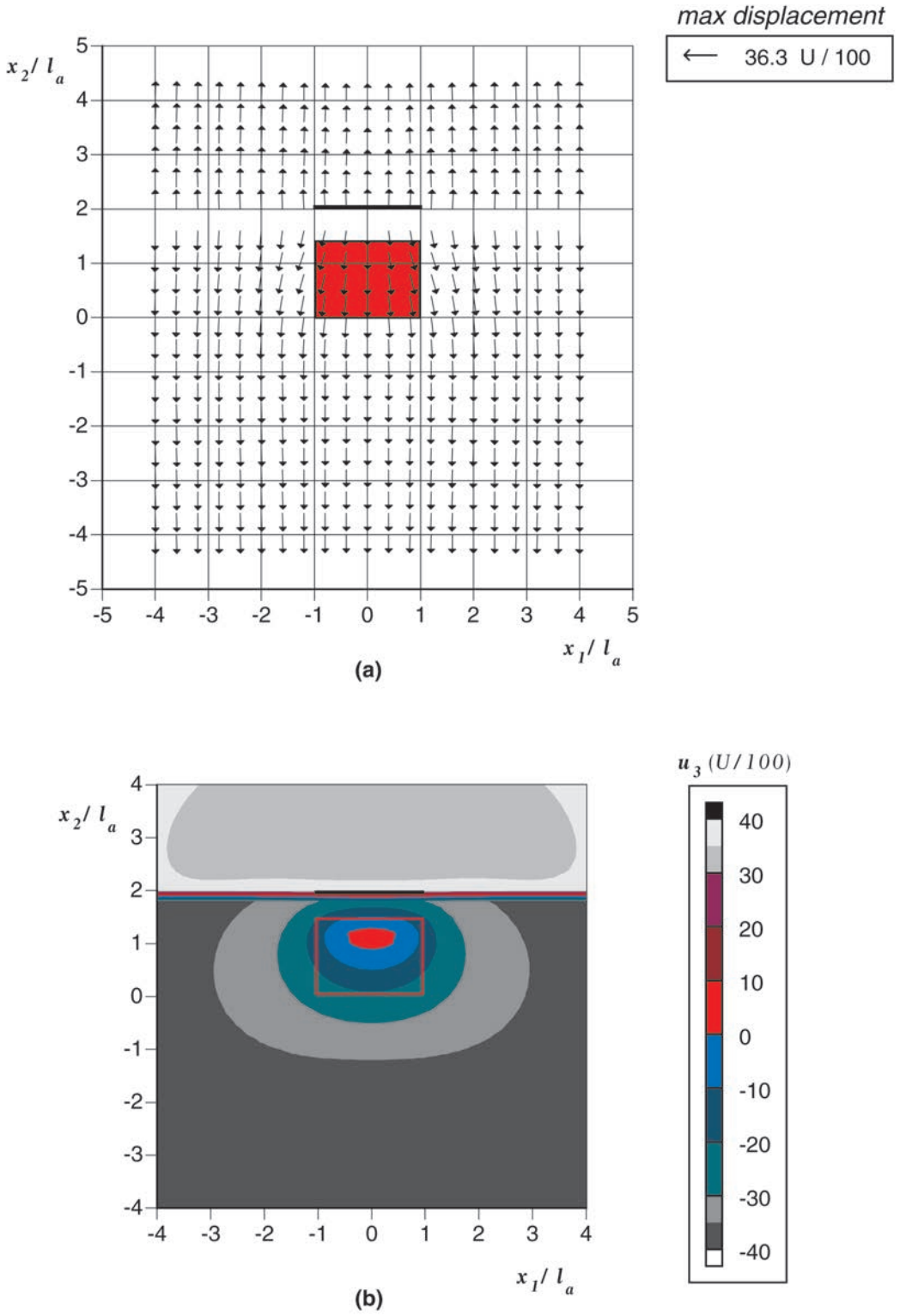

Fig. 6 - Maps of horizontal (a) and vertical displacement (b) in the case of an asperity included in a half-plane dislocation: z = 10 km, δ = 45° and l_a = 5 km.

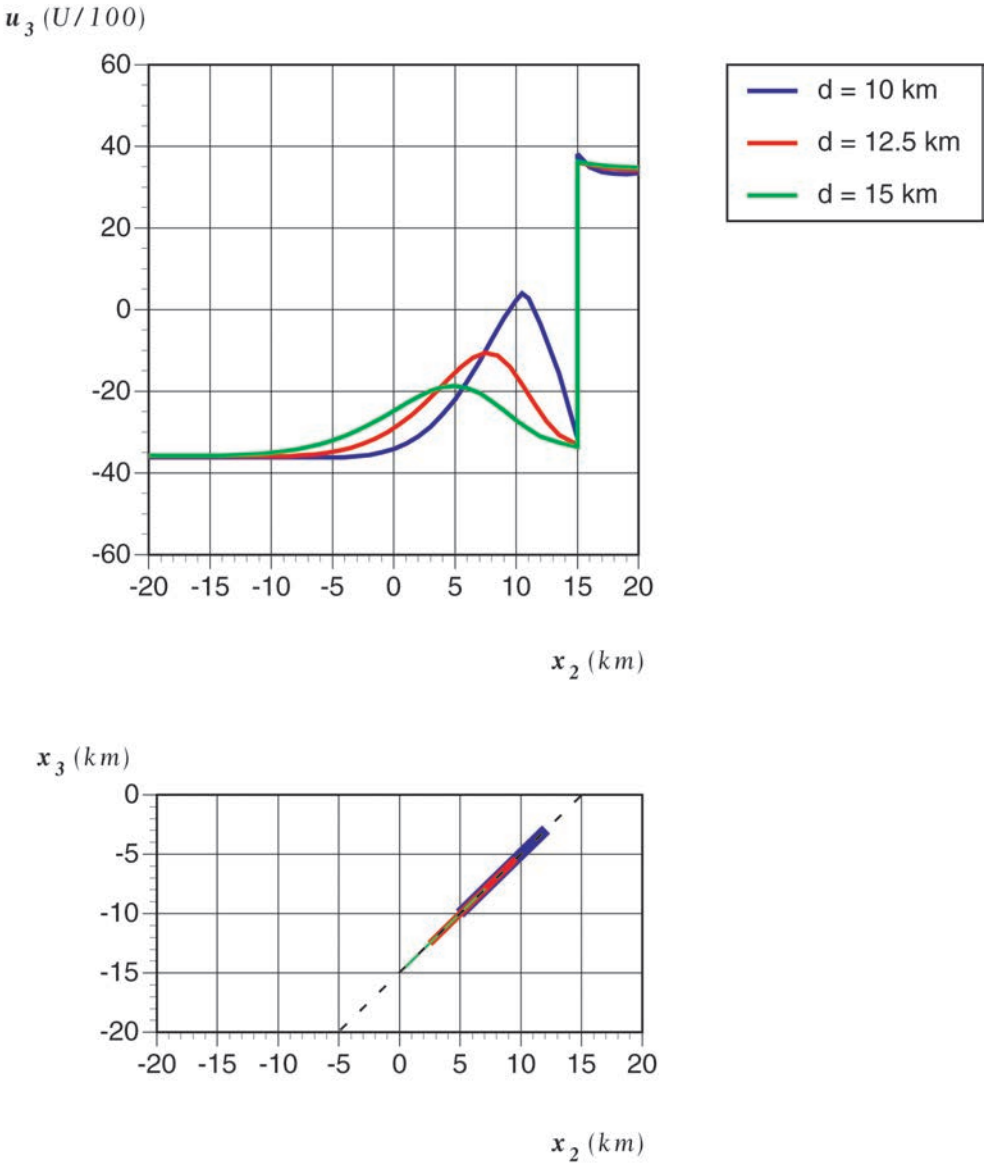

Fig. 7 - Vertical displacement u_3 for different values of d, in the case of a half-plane dislocation: $l_a = 5$ km and $\delta = 45°$.

To describe the observed surface deformation, it is interesting to evaluate the effects of the variation of model parameters on the ground displacement pattern. In particular, variations of the model parameters induce changes in the u_3 curves: an increase in asperity depth causes both a decrease in the maximum value of u_3 and an increase in the distance between fault trace and the position of maximum (Fig. 7); an increase in dip angle causes both a decrease in the maximum and a decrease in the distance between fault trace and maximum position (Fig. 8); an increase in asperity area causes both an increase in the maximum and a decrease in the distance between fault trace and maximum position (Fig. 9). Obviously, the ground displacement increases as the size of the asperity increases and its depth decreases.

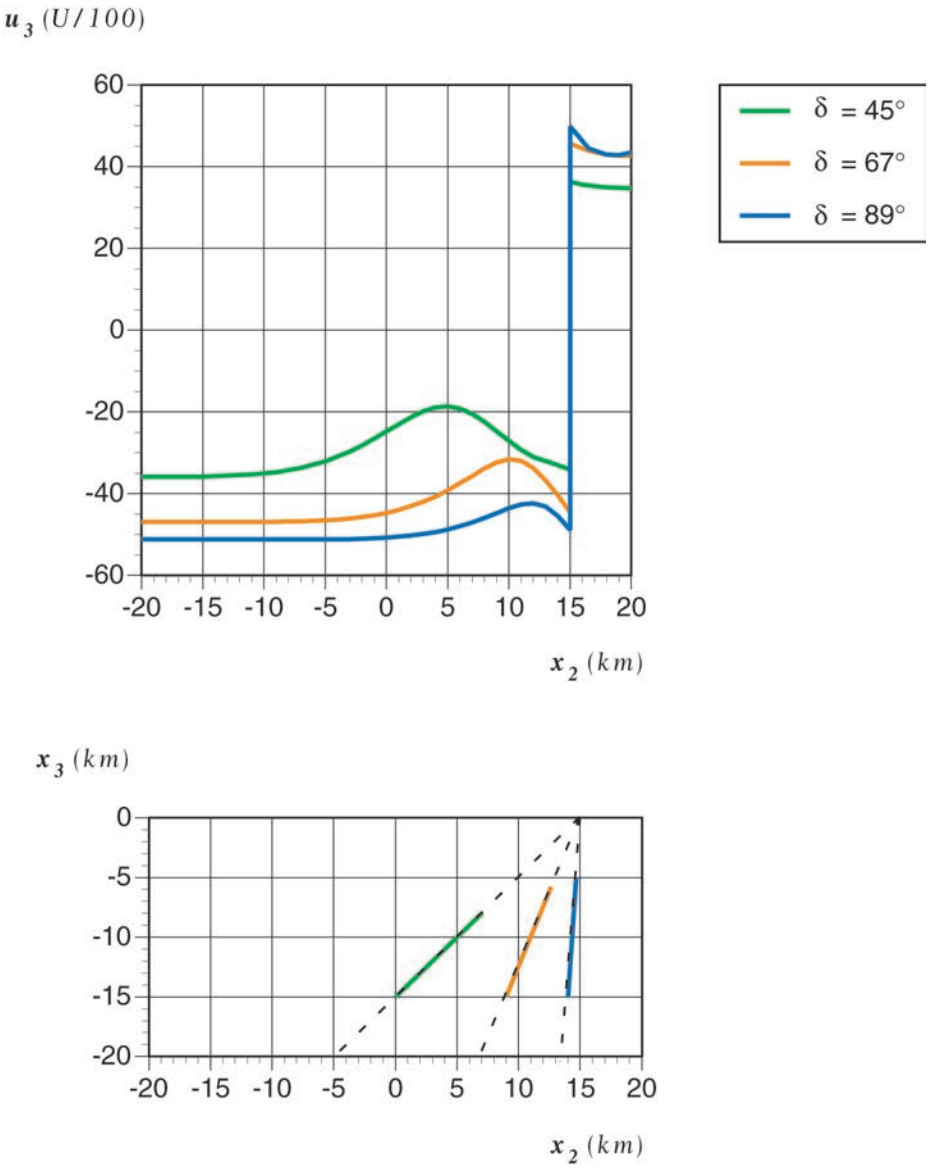

Fig. 8 - Vertical displacement u_3 for different values of angle δ, in the case of a half-plane dislocation: d = 15 km and l_a = 5 km.

For a fault dip of 45°, Fig. 10 shows vertical displacement for an asperity with l_a = 2.5 km, inside a concentric dislocation with side length increasing up to the Earth's surface and z = 15 km; we note that a larger side of the dislocation causes a larger vertical ground displacement and a shift of position of its maximum and minimum.

Fig. 11 shows the tilt fields along the x_2 axis for the cases shown in Fig. 4; the dashed line indicates the curve of the difference between the two cases. For U = 50 cm tilts of several μrad are produced. This indicates that the presence of an asperity on the fault plane can be appreciated also by tilt measurements.

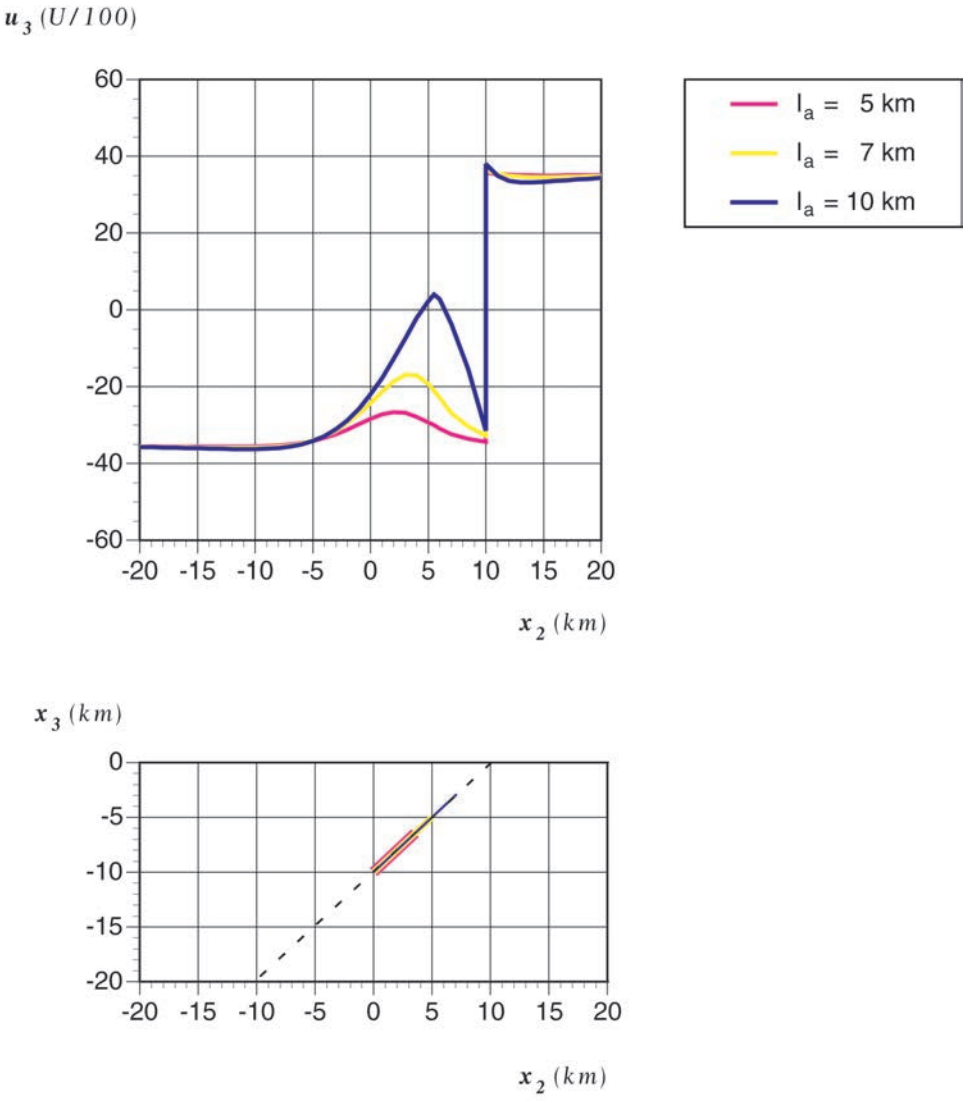

Fig. 9 - Vertical displacement u_3 for different values of l_a, in the case of a half-plane dislocation: d = 10 km and $\delta = 45°$.

The location of an asperity on a fault by geodetic measurements may allow us to evaluate the seismogenic potential of the asperity itself. In fact, we can define a potential seismic moment M_p of the asperity as the maximum value of the seismic moment that can be released in the failure of the asperity, calculated as

$$M_p = \mu A U \tag{8}$$

where μ is the rigidity of the elastic medium, A is the area of the asperity and U is the slip of the

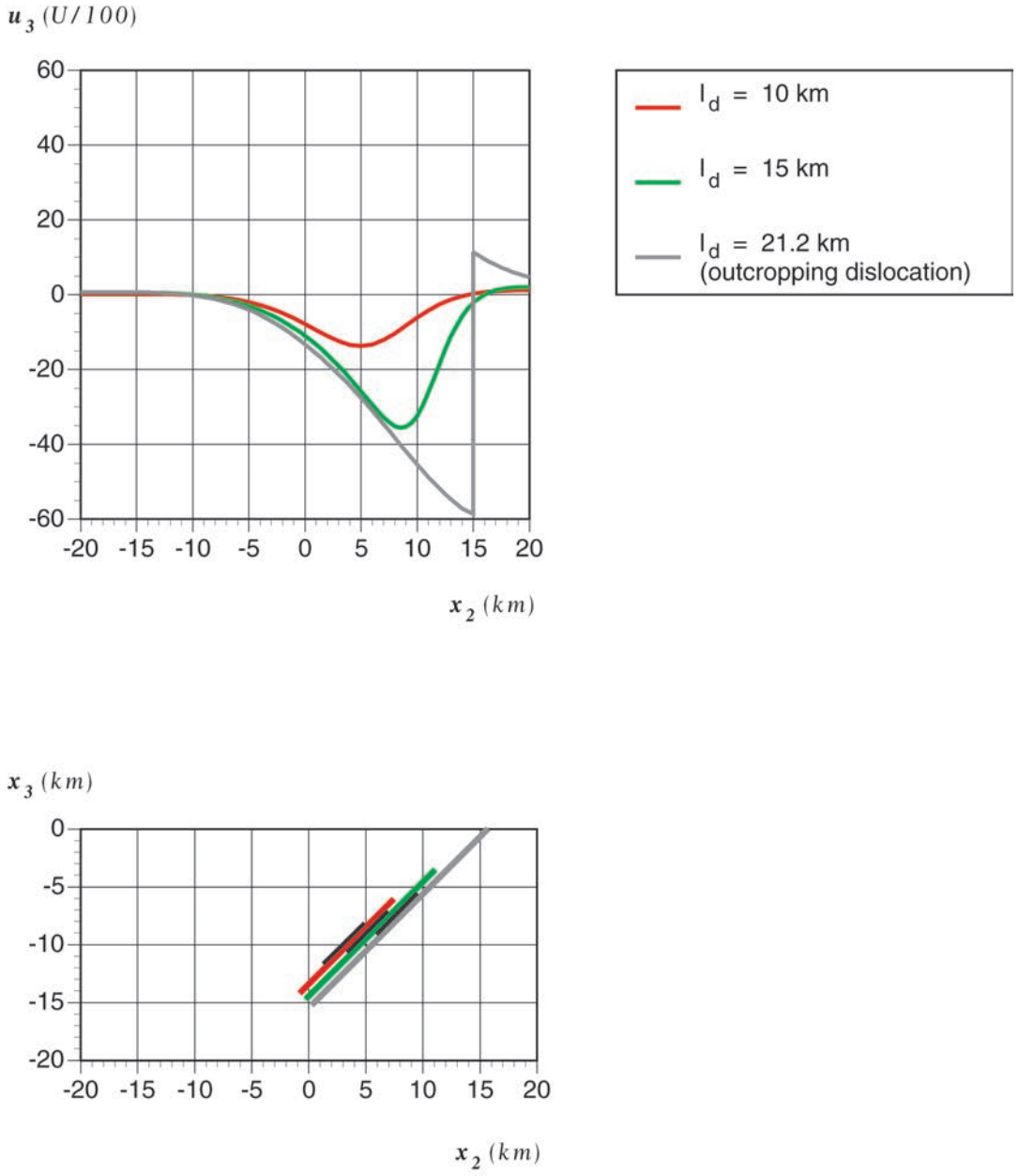

Fig. 10 - Vertical displacement u_3 for a finite-area dislocation in presence of an asperity for different values of l_d: z = 15 km, δ = 45° and l_a = 2.5 km.

surrounding fault area. The seismic moment M_p is released if during the earthquake the asperity slips by an amount U, so that the total displacement is uniform on the fault after the earthquake. With l_a= 2.5 km and U = 50 cm, we have $M_p = 1.5 \times 10^{18}$ N m, which corresponds to a magnitude-6 earthquake according to empirical relations (e.g. Kasahara, 1981).

The actual seismic moment may be greater than the value given in Eq. (8) if a larger area than

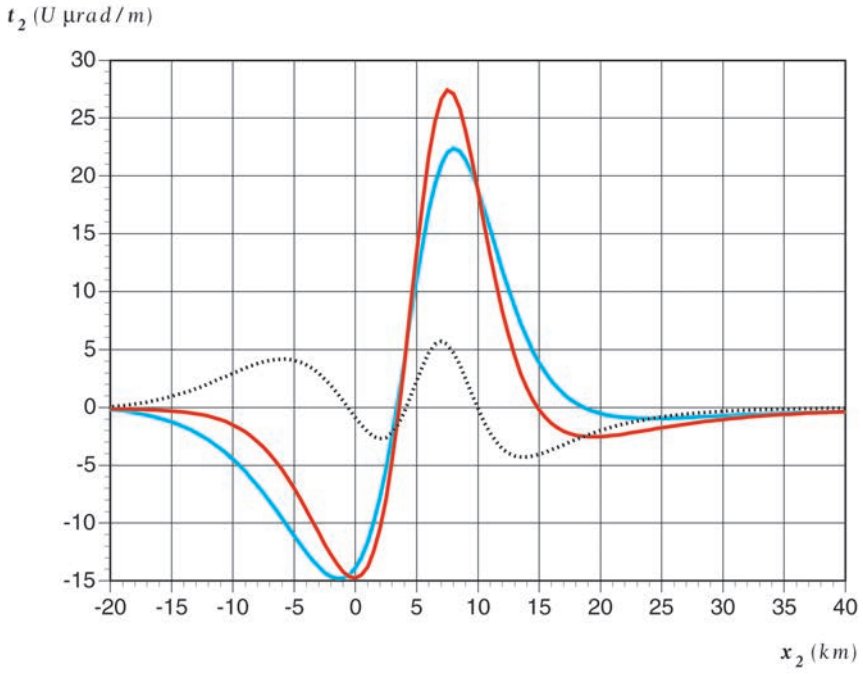

Fig. 11 - Tilt component t_2 along the x_2 axis the case of Fig. 4; the dashed line is the difference between the two curves.

the asperity ruptures during the earthquake. In the Parkfield segment of the San Andreas fault, for which accurate data are available, asperities with sizes in the order of several kilometres have been detected (Stuart et al.,1985; Harris and Segall, 1987).

4. Conclusions

Using leveling, GPS and InSAR data, it is now possible to study regional deformation fields and even to zoom in on individual faults. Geodetic measurements allow us to produce a complete picture of the ground displacement field. Post-seismic deformation studies exemplify how geodetic data are essential to understanding the aseismic fault behavior and the process of strain accumulation and release in a seismogenic region. Combining seismic and geodetic data should allow identification and characterization of active faults.

The model presented in this paper suggests how the displacement at the Earth's surface can be affected by the presence of asperities on active faults. The displacement and tilt fields can be very complex even in the case of relatively simple asperity shapes as considered in this paper. The inversion and the interpretation of geodetic measurements can give information about the depth, dip angle and area of the asperities, the amount of the aseismic fault slip and the potential seismic moment of the asperity. The interpretation of geodetic data with the present model starts from knowledge of the position and the orientation of the fault. This indicates that reliable interpretations can be given only in the presence of sufficiently dense geodetic networks.

We have shown that asperities, the failure of which can produce potentially damaging earthquakes (i.e. shallow asperities producing earthquake magnitudes ≥ 6), can be detected by accurate geodetic measurements.

Acknowledgments. This research has been carried out in the framework of grant ARS-98-68 of the Agenzia Spaziale Italiana.

References

Bakun W. H. and Lindh A. G.; 1985: *The Parkfied, California, prediction experiment*. Earthq. Predict. Res., **3**, 285-304.

Dragoni M.; 1988: *Role of geodetic measurements in the detection of fault asperities*. In: P. Baldi and S. Zerbini (eds), Proc. Third Int. Conf. on the WEGENER/MEDLAS Project, Bologna, 129-146.

Harris R. A. and Segall P.; 1987: *Detection of a locked zone at depth on the Parkfield, California, segment of the San Andreas Fault*. J. Geophys. Res., **92**, 7945-7962.

Kasahara K.; 1981: *Earthquake mechanics*. Cambridge Earth Science Series, Cambridge University Press, Cambridge, 248 pp.

Okada Y.; 1985: *Surface deformation due to shear and tensile faults in a half-space*. Bull. Seism. Soc. Amer., **75**, 1135-1154.

Slawson W. F. and Savage J. C.; 1983: *Deformation near the junction of the creeping and locked segments of the San Andreas Fault, Cholame Valley, California (1970-1980)*. Bull. Seism. Soc. Amer., **73**, 1407-1414.

Stuart W. D., Archuleta R. J. and Lindh A. G.; 1985: *Forecast model for moderate earthquakes near Parkfield, California*. J. Geophys. Res., **90**, 592-604.

Stuart W. D. and Tullis T. E.; 1995: *Fault model for preseismic deformation at Parkfield, California*. J. Geophys. Res., **100**, 24 079-24 099.

Tse S. T., Dmowska R. and Rice J. R.; 1985: *Stressing of locked patches along a creeping fault*. Bull. Seism. Soc. Amer., **75**, 709-736.